

Journal of Thermal Stresses



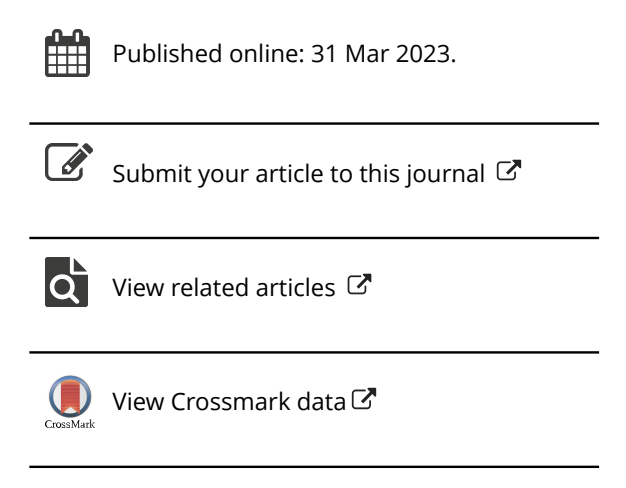
ISSN: (Print) (Online) Journal homepage: https://www.tandfonline.com/loi/uths20

Thermomechanical instability of viscoelastic friction materials in automotive disk clutches and brake pads

Kingsford Koranteng, Yizhan Zhang, Cortney LeNeave & Yun-Bo Yi

To cite this article: Kingsford Koranteng, Yizhan Zhang, Cortney LeNeave & Yun-Bo Yi (2023): Thermomechanical instability of viscoelastic friction materials in automotive disk clutches and brake pads, Journal of Thermal Stresses, DOI: 10.1080/01495739.2023.2191671

To link to this article: https://doi.org/10.1080/01495739.2023.2191671







Thermomechanical instability of viscoelastic friction materials in automotive disk clutches and brake pads

Kingsford Koranteng (D., Yizhan Zhang, Cortney LeNeave (D., and Yun-Bo Yi (D.)

Department of Mechanical and Materials Engineering, University of Denver, Denver, Colorado, USA

ABSTRACT

The objective of this study is to develop a mathematical model to aid in predicting the onset of instability in automotive disk brakes and clutches when using viscoelastic friction materials. The model is derived from and expands upon the fundamental of Burton's model for thermoelasticity in pure elastic materials. In this investigation, three physical material parameters are considered: relaxation time, elasticity, and thermal conductivity. Prior to this parametric study, the effects of these material properties in relation to thermoelasticity were yet to be fully understood. Therefore, a finite element analysis is developed and used to validate the mathematical model by comparing the variation of the critical speed as a function of thermal conductivity. The results reveal that an increase in the relaxation time significantly reduces the critical sliding speed. Changing the elastic parameter further increases the effect of relaxation time by also reducing the critical sliding speed. However, increasing the thermal conductivity parameter dampens the effect of the elastic parameter and relaxation time on the critical speed. The study concludes there is a critical value of the relaxation time and elastic parameter above which the system stability is improved, meanwhile thermal conductivity attempts to counter the stability gained from other material properties. The study is instrumental in understanding the influence of viscoelastic parameters in sliding systems and provides an intuitive means of predicting the onset of thermomechanical instability.

ARTICLE HISTORY

Received 19 September 2022 Accepted 27 February 2023

KEYWORDS

Brake pad/clutch disk; critical speed; friction; thermomechanical; viscoelasticity

1. Introduction

It is widely known that the sliding interactions between the friction ring section of a rotating disk (rotor) and the brake/clutch lining material are usually accompanied by vibrations. The vibration occurring at the interface between these two sliding materials tends to excite the entire rotor creating unwanted noise. This noise is transmitted to other parts of the vehicle, and unfortunately the occupants of the vehicle may experience discomfort due to these vibrations. The noise generated is more intense with the use of metallic and semi-metallic brake lining materials [1, 2]. In an attempt to address these challenges, manufacturers have embraced a somewhat innovative approach where damping elements are applied to the backing plate of the brake assembly to reduce noise transmission [3]. An example of such an invention is a laminate that includes one or two layers of viscoelastic adhesives, bonded to one or more intermediate materials to form the brake pad assembly.

Research has proven that the vibration and noise in brake systems can be dissipated by using material damping in the brake components [4-6]. However, it is interesting to note that the application of damping materials to the backplate does not adequately reduce the unwanted noise transmitted to the occupant of the vehicle [7]. This is expected because the noise and vibration generated due to thermomechanical instabilities occur at the interface of the sliding pairs and not at the backing plate. Therefore, the most effective approach to reducing noise and vibration in brake systems is to consider a special class of friction materials with acceptable thermophysical parameters, stable friction coefficient, optimal elastic behavior, and damping properties as proposed by Sergienko et al. [8]. Meanwhile, there are few published studies on how such materials could impact brake performance. This article considers a low viscoelastic material as a friction lining in an automotive disk brake pad, and investigates how the physical material properties could influence the onset of thermomechanical instabilities, as these types of materials are known to eliminate noise, vibration, and squeal in sliding systems [3, 9]. When solid bodies come into contact under the influence of an applied load, contact stresses develop at the contact interface which is influenced by temperature in the case of sliding. In the process, peak values of the contact stresses cause thermomechanical instability to occur [10]. To minimize or prevent this phenomenon, a reduction of the peak values of the contact stresses are targeted to make the interface pressure as uniform as possible. Based on the mechanism of contact systems and the nature of viscoelastic materials, reduced pressure peak values can be attained [11]. Currently, there is no comprehensive experimental or theoretical study on viscoelastic friction materials and how they excite thermomechanical instability in automotive disk brakes and clutches, except for the limiting case considered by Decuzzi [12]. The authors developed an analytical model to study the effect of viscoelastic and poroelastic properties of friction materials on the onset of frictionally excited thermoelastic instability. The model was restricted to materials with zero thermal conductivity and therefore assumes that the critical sliding speed of the pure metallic material is completely zero, while that of the viscoelastic material is equal to the sliding speed. This results in the over-approximation of the critical sliding speeds, tending to predict a much higher instability for real materials. More importantly, the model does not provide an efficient means of obtaining the critical sliding speed of both sliding materials simultaneously.

It is imperative to note that there are several research works on the contact interactions of solids involving viscoelastic materials, but only a few focused-on surface interfacial behavior and how it influences sliding instability. Yu et al. [13] derived viscoelastic contact models for a more realistic contact analysis and also developed a model based empirical method to determine the localized properties of a viscoelastic material. Furthermore, the influence of material dependent damping on brake squeal in disk brake systems has been numerically and experimentally studied by Úradníček et al. [14]. The authors found that nonproportional material dependent damping can significantly affect the stability of the brake system. Zhao et al. [15] carried out an important study on the friction analysis of an anisotropic surface by considering a viscoelastic material. This was an extension of Persson's [16, 17] work to study sliding friction and the effect of the elastic modulus on the contact area. Also, Feng et al. [18] carried out a study to establish the relations between viscoelastic friction and wear by considering a polymer composite friction lining materials and wire rope.

The work herein derives a mathematical model, which uses a numerical approach to predict the critical sliding speed of friction material with viscoelastic parameters. Materials with viscoelastic properties are widely used in the automotive industry because of their ability to dissipate noise and vibrations from systems. This investigation studies the response of viscoelastic material to thermomechanical instability when used as friction materials in brake pads and clutch disks as a means of controlling noise and vibration. The work does not consider the frequency response and its resulting vibration and noise effect during sliding interaction but rather the response of the viscoelastic parameters to thermomechanical instability. The main objective of this study and

a major distinction between this and prior work is that the model predicts the critical sliding speed for both the viscoelastic friction material and the pure elastic material during sliding by considering the thermal conductivity parameters unlike the limiting case considered by Decuzzi [12], where the thermal conductivity of the friction material is assumed to be zero. Moreover, this work seeks to foster the idea of using viscoelastic friction materials for brake pads and disk clutches.

2. The mathematical formulation of the problem

Multiple models have been established to describe the behavior of viscoelastic materials. However, the simplest model which adequately predicts this behavior, and is widely used in solid mechanics, is the standard linear solid model also known as the three-parameter model [19]. The three-parameter model is established by either adding a spring in series or parallel to a Maxwell model [20]. The Maxwell model consists of a spring and dashpot connected in series. In this work, a spring placed in parallel with a series connection of a spring and a dashpot is considered to represent the viscoelastic model, shown in Figure 1. The physical model, which consists of a viscoelastic friction material and a steel disk, is treated as two straight blades on a single plane, in contact along a straight common interface, as shown in Figure 2. The model does not consider thermal radiation nor thermal convection heat exchange with the surrounding air. The fundamental mathematical derivation, which describes the thermomechanical behavior was obtained from Burton et al. [21].

If the linearly viscoelastic plate designated as body 1 is loaded with a sinusoidal pressure, the strain response is also sinusoidal with the same frequency as the applied pressure but lags by a phase angle δ . Thus,

$$\varepsilon_1 = \varepsilon_0 \cos\left(\omega x - \delta\right) \tag{1}$$

where ε_0 is a constant. Moreover, Eq. (1) can be rewritten as

$$\varepsilon_1 = \varepsilon_0 e^{i(\omega x - \delta)} \Rightarrow \varepsilon_0 e^{i\omega x} e^{-i\delta}$$
(2)

Considering the linear elastic plate designated as body 2, the strain response does not lag as in the case of the viscoelastic material and can be expressed as:

$$\varepsilon_2 = \varepsilon_0 e^{i(\omega x)} \Rightarrow \varepsilon_0 e^{i\omega x}$$
 (3)

From Burton's equation [21], it follows that the surface pressure on bodies 1 and 2, with the surface held flat, can be expressed as Eq. (4) and Eq. (5) respectively:

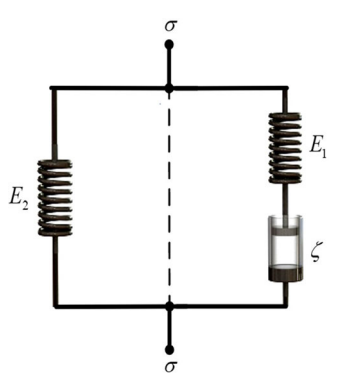


Figure 1. Standard solid model describing the viscoelastic behavior.

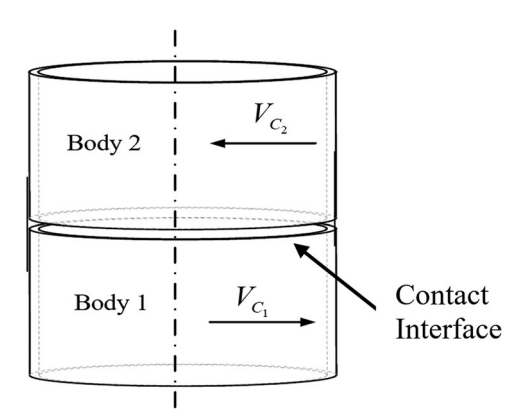


Figure 2. Geometry configuration of sliding bodies.

$$P_{1}^{'} = \frac{E_{1}\alpha_{1}T_{0}k_{1}}{V_{c_{1}}} \left[-\left(\omega - b_{1}\right)\cos\left(\omega x\right) + a_{1}\sin\left(\omega x\right) \right]$$

$$\tag{4}$$

$$P_{2}^{'} = \frac{E_{2}\alpha_{2}T_{0}k_{2}}{V_{c_{2}}} \left[\left(\omega - b_{2}\right) \cos(\omega x) + a_{2}\sin(\omega x) \right]$$
 (5)

Here:

$$a_{i} = \left[-\frac{\omega^{2}}{2} + \frac{\omega}{2} \left\{ \omega^{2} + \left(\frac{V_{c_{1}}}{k_{1}} \right)^{2} \right\}^{\frac{1}{2}} \right]^{\frac{1}{2}} \text{ and } b_{i} = \left[\frac{\omega^{2}}{2} + \frac{\omega}{2} \left\{ \omega^{2} + \left(\frac{V_{c_{1}}}{k_{1}} \right)^{2} \right\}^{\frac{1}{2}} \right]^{\frac{1}{2}}, i = 1, 2$$

When the two bodies are in contact, each surface is expected to undergo equal and opposite displacement. If we consider a cosine wave distribution of the displacement, the pressure on body 1 can be expressed as $P = P_1' - P_1''$. where

$$\ddot{P_1} = -\frac{E_1 \omega \varepsilon_1}{2} \Rightarrow -\frac{E_1 \omega \varepsilon_0 e^{i\omega t} e^{-i\delta}}{2} \tag{6}$$

For body 2, the pressure on the body is given as $P = P_2^{'} - P_2^{''}$. Where:

$$P_2^{"} = \frac{E_2 \omega \varepsilon_2}{2} \Rightarrow \frac{E_2 \omega \varepsilon_0 e^{i\omega t}}{2} \tag{7}$$

By considering the equilibrium condition, where pressure, P is identical on both bodies. We can express P as:

$$P = \frac{E_1 P_2' + E_2 P_1' e^{-i\delta}}{E_1 + E_2 e^{-i\delta}}$$
 (8)

By substituting $P_1^{'}$ and $P_2^{'}$ into Eq. (8), we obtain:

$$P = \frac{E_{1}E_{2}T_{0}}{E_{1} + E_{2}e^{-i\delta}} \begin{bmatrix} \left(\frac{\alpha_{1}k_{1}(b_{1} - \omega)e^{-i\delta}}{V_{c_{1}}} - \frac{\alpha_{2}k_{2}(b_{2} - \omega)}{V_{c_{2}}}\right)\cos(\omega x) + \\ \left(\frac{\alpha_{1}a_{1}k_{1}e^{-i\delta}}{V_{c_{1}}} + \frac{\alpha_{2}a_{2}k_{2}}{V_{c_{2}}}\right)\sin(\omega x) \end{bmatrix}$$
(9)

Meanwhile, for equilibrium, the heat generated due to friction must equal heat conducted from the interface.

$$\mu P(V_{c_1} + V_{c_2}) = q_{\text{net}} \tag{10}$$

where $q_{\rm net}$ is the net heat flow between the bodies as expressed in Eq. (11). Reference to the derivation can be found in Burton et al. [21].

$$q_{\text{net}} = q_1 + q_2 = T_0 \{ (K_1 b_1 + K_2 b_2) \sin(\omega x) + (K_2 a_2 - K_1 b_1) \cos(\omega x) \}$$
(11)

Substituting Eqs. (9) and (11) into Eq. (10). We get:

$$\frac{\mu E_{1} E_{2}(V_{c_{1}} + V_{c_{2}})}{E_{1} + E_{2} e^{-i\delta}} \begin{bmatrix} \left(\frac{\alpha_{1} k_{1}(b_{1} - \omega) e^{-i\delta}}{V_{c_{1}}} - \frac{\alpha_{2} k_{2}(b_{2} - \omega)}{V_{c_{2}}}\right) \cos(\omega x) \\ + \\ \left(\frac{\alpha_{1} a_{1} k_{1} e^{-i\delta}}{V_{c_{1}}} + \frac{\alpha_{2} a_{2} k_{2}}{V_{c_{2}}}\right) \sin(\omega x) \end{bmatrix}$$

$$= (K_{1} b_{1} + K_{2} b_{2}) \sin(\omega x) + (K_{2} a_{2} - K_{1} b_{1}) \cos(\omega x) \tag{12}$$

where $e^{-i\delta} = (\cos \delta - i\sin \delta)$. Note that, $i\sin \delta$ is the imaginary component.

Rearranging the coefficients of the sine and cosine terms to be equal on both sides of Eq. (12) gives:

$$\frac{\mu E_1 E_2 (V_{c_1} + V_{c_2})}{E_1 + E_2 (\cos \delta)} \left[\left(\frac{\alpha_1 k_1 (b_1 - \omega) (\cos \delta)}{V_{c_1}} - \frac{\alpha_2 k_2 (b_2 - \omega)}{V_{c_2}} \right) \right] = (K_2 a_2 - K_1 b_1)$$
(13)

$$\frac{\mu E_1 E_2 (V_{c_1} + V_{c_2})}{E_1 + E_2 (\cos \delta)} \left[\left(\frac{\alpha_1 a_1 k_1 (\cos \delta)}{V_{c_1}} + \frac{\alpha_2 a_2 k_2}{V_{c_2}} \right) \right] = (K_1 b_1 + K_2 b_2)$$
(14)

Equations (13) and (14) are solved using numerical techniques, such as Gaussian elimination to obtain V_{C_1} and V_{C_2} for the viscoelastic friction material and the steel material respectively.

To obtain the expression for the phase lag, the standard linear model consisting of a spring E_2 in parallel to a series connection of a spring E_1 and a dashpot ζ , displayed in Figure 1, as obtained in Findley et al. [22] is used. The expression is given as:

$$\delta = -\arctan\left(\frac{\omega \varsigma E_2^2}{(E_1 + E_2)\omega^2 \varsigma^2 + E_1 E_2^2}\right) \tag{15}$$

where the load frequency, ω is given as:

$$\omega = \frac{Vm}{2\pi} \tag{16}$$

where $V = V_{C_1} + V_{C_2}$ is the sliding velocity and m is the wave number of the imposed perturbation.

3. Finite element approach

To validate the derived expressions for the critical speed of the viscoelastic friction material siding against the metal material, a finite element model is utilized. Two plates that are thermally conducting are used. Plate 1 is the viscoelastic material that moves in-plane with a sliding velocity V with respect to plate 2, the conducting material. Plate 1 moves in the x and y direction while plate 2 is constrained in the x and y directions. Figure 3 shows a schematic of the sliding bodies used in this study. The two plates have equal lengths L and heights of h_1 and h_2 respectively.

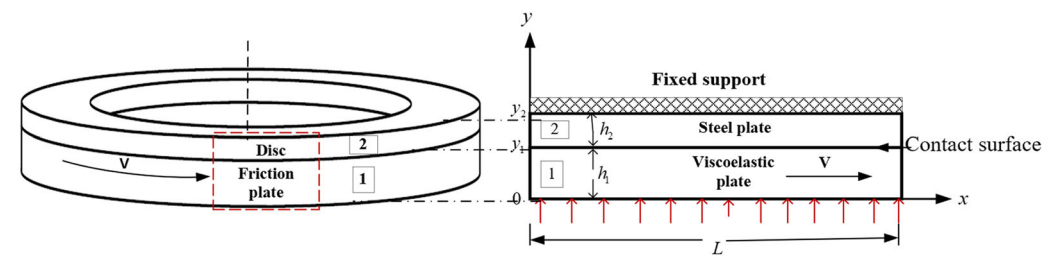


Figure 3. Schematic of the two sliding bodies.

Where $y = y_1$ represents the contact interface between the two plates. Reference to the applied boundary conditions, mesh refinement procedures and the accuracy of the model can be obtained from Koranteng et al. [23].

Throughout this analysis, the commercial finite element package ABAQUS [24], which is equipped with the Petrov-Galerkin algorithm, is utilized. A viscoelastic analysis comprised of a single Maxwell model is considered. The viscoelastic parameters shear modulus, bulk modulus, and the relaxation time $\tau = \varsigma/E_1$ are computed and applied using an ABAQUS input script.

3.1. Solution procedure for the viscoelastic model

The following list outlines the procedure used in this study to solve the viscoelastic model.

1. Impose a sinusoidal perturbation having a specific wavenumber $(m = 2n\pi/L)$ onto a mean contact pressure as:

$$p(x,t) = P_m + A\sin(\omega x - \delta) \tag{17}$$

Here, a sinusoidal load is used because it provides a more convenient way to get a response from viscoelastic materials under a short time loading when compared to using a static load [22]. Further, the frictional heat at the contact interface $y = y_1$ is computed using the pressure in Eq. (17), the sliding velocity, and the friction coefficient value. We defined a mass flow onto the moving body using the density, ρ of the moving body, and the sliding velocity, V. These are applied in ABAQUS via a user-defined Subroutine.

- 1. A heat transfer analysis is carried out and the resulting nodal temperatures are extracted from the contacting interface at $y = y_1$. The nodal temperatures are fed into a dynamic viscoelastic step in ABAQUS.
- 2. The contact pressure resulting from the viscoelastic analysis is extracted from the sliding interface. The new nodal contact pressure is used to compute the heat flux for the next heat transfer analysis.
- 3. Repeat the process using an iterative scheme as shown in the simulation procedure in Figure 4. For each iteration, extract the maximum contact pressure or temperature, while taking note of the time steps involved.
- 4. Find the natural log of the values from step 4 and plot a graph of the natural log of the contact pressure or temperature versus time. The plot is linear with either a positive or negative slope. The slope represents the growth rate of the perturbation. For a positive slope, which indicates instability, $V > V_{C_1}$ and for a negative slope which indicates stability within the system, $V < V_{C_1}$. Since the critical speed is initially unknown, the sliding speed can be adjusted while observing the resulting maximum temperature or contact pressures at each iteration.

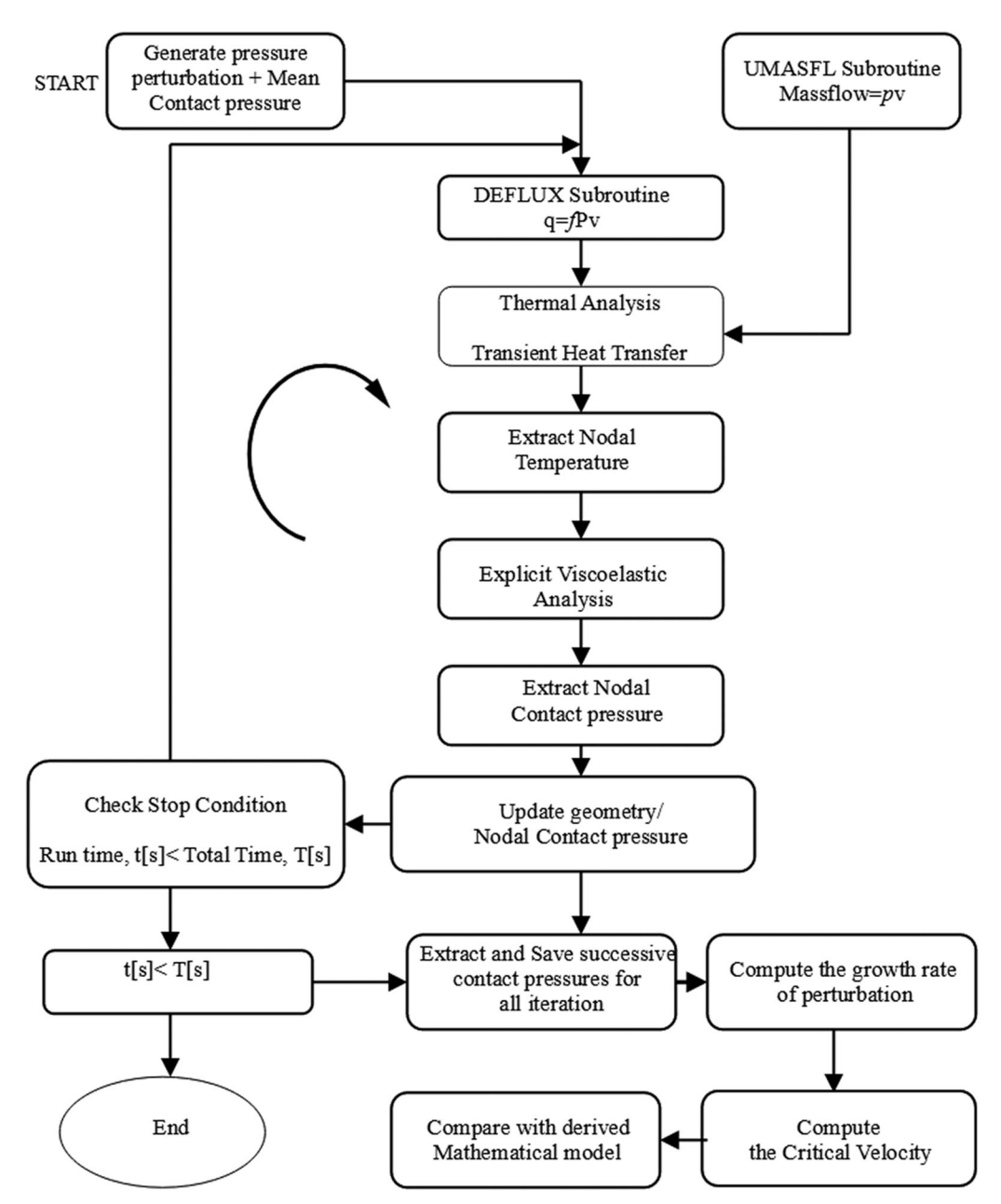


Figure 4. Simulation solution procedure.

The critical speed is obtained using a linear interpolation procedure based on the condition that the critical speed occurs when the growth rate, b is zero. For a stable system, the critical sliding speed needs to be high. Meanwhile, a reduced critical sliding speed implies that the system is unstable.

3.2. Convective term and convergence problem

Solutions to conductive-convective problems are usually accompanied by numerical errors due to convergence issues. These numerical convergence issues usually occur when the Peclet number exceeds 2. Typically for clutch and brake problems, the Peclet number is greater than 100. Also, when using the standard Galerkin finite element procedure, results are anticipated to have high numerical errors. Therefore, ABAQUS [22], a commercial finite element package equipped with a Petrov-Galerkin algorithm to handle the conductive convective problem, is utilized in this investigation. The algorithm uses an up-winding approach [25, 26], where the central-difference scheme is replaced with the backward-difference scheme for the conductive-convective term. Further, the high Peclet number associated with the brake/clutch model is due to the imposed perturbation moving at a fast speed close to the sliding velocity, with respect to the poor conductor. This causes a high temperature gradient, in the y-direction, near the contact surface of the poor conductor [18, 19]. To address this problem, the finite element mesh of the poor conductor is biased at 1.25 near the contact surface and a mesh refinement exercise ensures the model is capable of reproducing a strong variation of temperature in the skin layer by estimating the temperature distribution perpendicular to the interface [27] as shown in Figure 5.

3.3. Validation of the mathematical model

The results from Eqs. (13) and (14) are validated by comparing the effect of the thermal conductivity of the viscoelastic friction material on the critical sliding speed of the system with the results of the finite element simulations. Further, since it is difficult and expensive to perform experimental work on this study by considering the range of physical parameters used, the results are compared with Burton's model which is well-known and experimentally validated as shown in Figure 6a. Table 1 shows the material properties used in the analysis. The simulated finite element approach agrees quite well with the results from the derived mathematical model. Furthermore, the result from Burton's model is different from the other two models with viscoelastic parameters, but this is expected as the presence of a damping element in the two models may decrease the critical sliding speed depending on the viscoelastic parameters.

To further prove the accuracy of the model, a comparison between the Decuzzi model and the developed mathematical model is considered. To compare the two models, the thermal conductivity of the friction material in the developed model is set to zero, that is, $K_1 = 0$ since the Decuzzi model neglects the effect of thermal conductivity of the friction material. Moreover, since the developed model assumes that the surface displacement in the y-direction is zero, that is, $u|_{v=0}=0$, it implies that there will be no lateral expansion of the model and so Poisson's ratio ν_1 , is nearly zero. Therefore, the smaller the Poisson's ratio used in the Decuzzi model, the more it agrees well with the developed model. Figure 6b shows the comparison between the two models with a Poisson's ratio $\nu_1 \approx 0$. Note that a 1:1 ratio is obtained when $\nu_1 = 0$. The results from Figure 6a and b provide confidence in the output results from the developed mathematical expression for investigating the critical sliding speed of viscoelastic friction material.

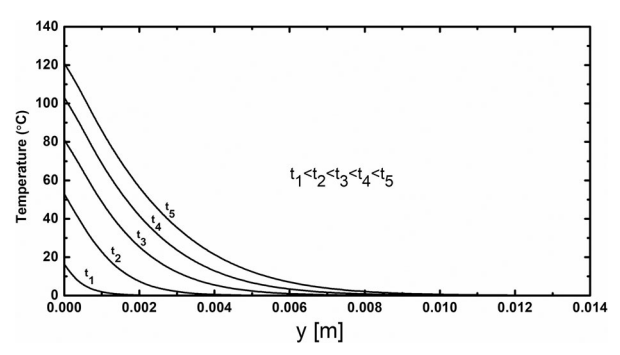


Figure 5. Character of temperature distribution in the skin layer of the finite element mesh of the poor conductor [23].

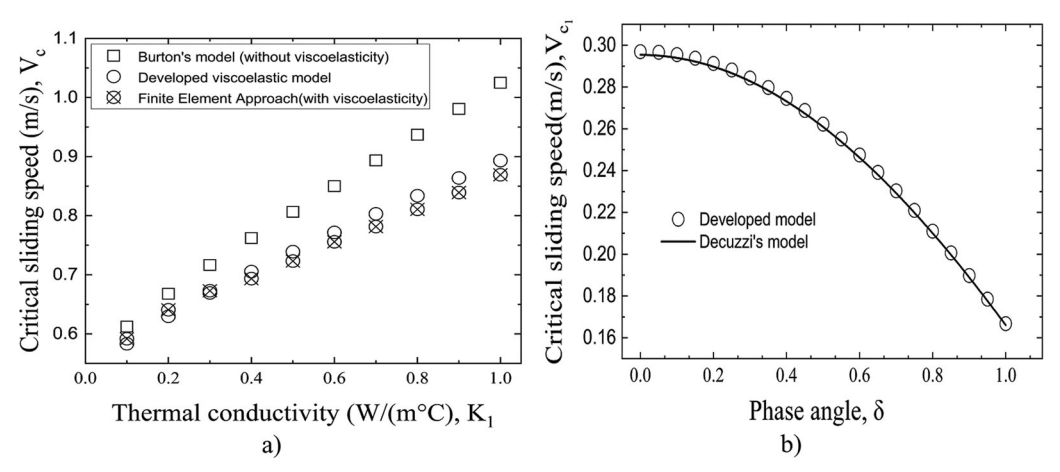


Figure 6. Comparison of the effect of (a) thermal conductivity and (b) phase angle on the critical sliding speed of the viscoelastic material for different models.

Table 1. Properties of the material used in the study.

Properties	Conducting material (steel)	Friction material
Modulus of elasticity, E (GPa)	210	6
Damping modulus (GPa)	_	0.2
Conductivity, K (W/(m·K))	57	0.1–1
Poisson's ratio, v	0.25	0.25
Thermal expansion coefficient, α (10 ⁻⁶ K ⁻¹)	12	14.2
Specific heat, $C(J \cdot kg^{-1} \cdot K^{-1})$	460	120
Density, ρ (kg/m ³)	7250	2000

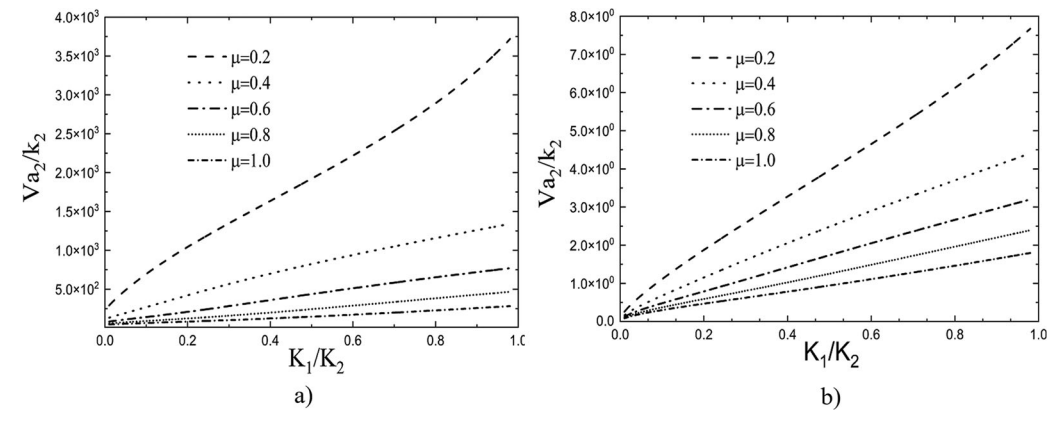


Figure 7. The variation of dimensionless critical speed as a function of the ratio of the thermal conductivities for (a) the viscoelastic friction material and (b) the pure elastic conducting material.

4. Results

The mathematical formulation is applied to investigate the variation of the normalized critical sliding speed with other physical material parameters by solving Eqs. (13) and (14) simultaneously using a numerical approach. The sliding speed V, and wave parameter are normalized in terms of the half-thickness of the metal material, a_2 , and its thermal diffusivity k_2 . Figure 7a and b show the variations of the dimensionless critical sliding speed in the viscoelastic friction material and the metal material respectively, by considering different ratios of the thermal

conductivities at different friction coefficient values. The wavenumber $m = 2\pi/L$ is 32, which represents an upper limit for actual sliding bodies.

The resulting normalized critical speed Va_2/k_2 in the viscoelastic material is significantly higher than that of the metal material when K_1/K_2 is varied from 0 to 1. This behavior, which is observed in the linear elastic model by Burton et al. [21] is preserved in the case of the viscoelastic model. When $\mu = 0.2$ for both materials, the curve departed significantly from the remaining μ plots. A deeper look reveals that, for even larger values of μ , the curves flatten with a considerably reduced critical speed. It can be inferred from the graphs that the effect of thermal conductivity is less dominant for larger values of μ . Thus, increasing μ decreases the critical sliding speed of the system and promotes the occurrence of noise and vibration which may lead to buckling, hot spots, thermal fatigue, etc. For stability purposes, an appropriate combination of the friction coefficient μ and thermal conductivities is required for sliding stability.

Figure 8a considers the dimensionless wave number and is essential in understanding the influence of the relaxation time $\zeta/E_1(K_1/K_2=0.02)$ on the system stability. It should be noted that the higher the value of ζ/E_1 , the greater the damping effect during sliding. For the pure elastic solution, where $\zeta/E_1=0$, the normalized critical speed Va_2/k_2 as a function of the wave parameter is linear and relatively high.

This indicates a more stable system but may not necessarily prevent noise and vibration over time. Besides, when $\zeta/E_1 > 0$, a nonlinear reduction in the critical sliding speed as a function of wave parameter, ma, is observed. This becomes more pronounced as ζ/E_1 is increased. Thus, it follows that the relaxation time decreases the effect of the wave parameter (ma > 0.2) on the critical speed. Figure 8b shows the variation of the dimensionless critical speed as a function of the wave parameter for different elastic parameters E_1/E_2 ($\zeta/E_1=0.02$). As the elastic parameter E_1/E_2 increases, the critical speed Va_2/k_2 reduces significantly. This clearly shows that increasing the elastic parameter E_1/E_2 reduces the effect of the wave parameter on the system stability. Therefore, when the ratio of the elasticity of the two sliding materials is relatively high, the system stability cannot be guaranteed. The variation of the normalized critical speed Va_2/k_2 as a function of the thermal conductivity parameter K_1/K_2 at different relaxation times ζ/E_1 and elastic parameters E_1/E_2 are considered in Figure 9. The effect of the relaxation time on the system stability as the thermal conductivity parameter K_1/K_2 is increased is very significant in Figure 9a. The overall critical speed decreases as the relaxation time increases. For instance, at $\zeta/E_1=0$, the resulting critical speed is found to be dominant. Further increasing ζ/E_1 causes the overall critical speed Va_2/k_2 to reduce slightly. Similarly, as the elastic parameter is increased in Figure 9b, the overall critical speed decreases. This means that increasing the relaxation time ζ/E_1 and elastic parameter decrease the effect of the thermal conductivity parameter and makes the system prone to instability.

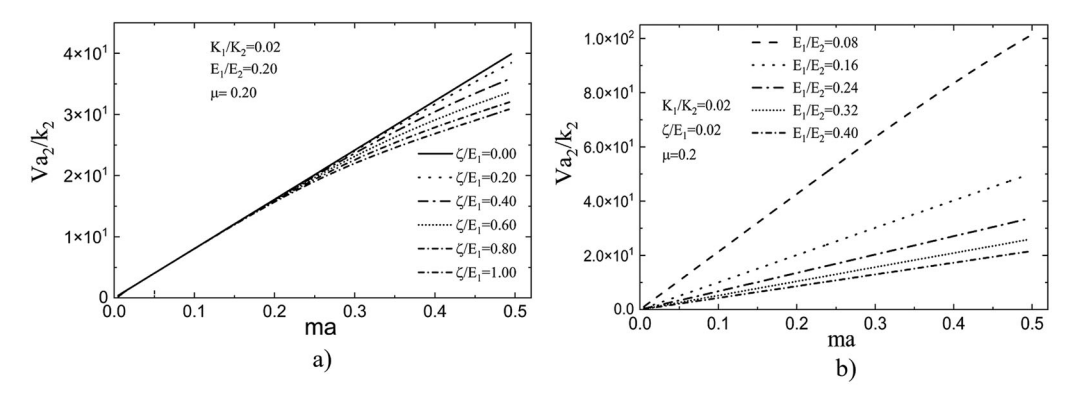


Figure 8. The variation of the dimensionless critical speed as a function of the wave parameter for (a) different values of the relaxation time, ζ/E_1 and (b) different values of the elastic parameter, E_1/E_2 .

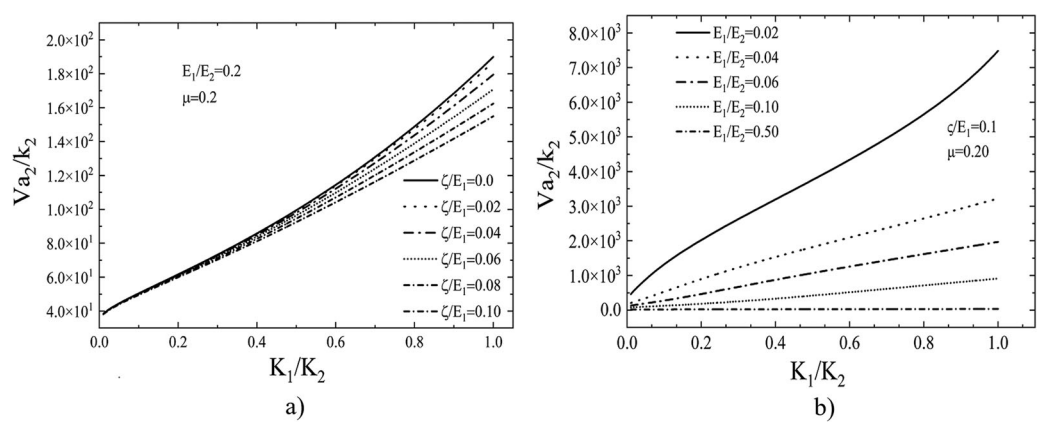


Figure 9. The variation of the dimensionless critical speed with the thermal conductivity parameters at different (a) relaxation time parameters, ζ/E_1 and (b) elastic parameters, E_1/E_2 .

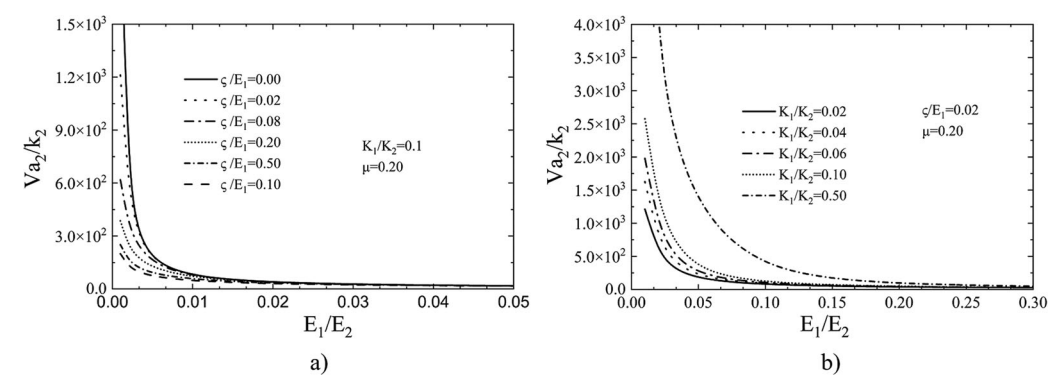


Figure 10. The variation of the dimensionless critical speed with the elastic parameter at different (a) relaxation time, ζ/E_1 and (b) thermal conductivity ratio, K_1/K_2 .

Figure 10a and b show the variation of the normalized critical speed Va_2/k_2 with the elastic parameter for different values of the relaxation time parameter ζ/E_1 and the thermal conductivity parameter K_1/K_2 respectively. The critical speed decreases rapidly as the elastic parameter E_1/E_2 is increased. This is intuitive because an increase in E_1/E_2 leads to high stress levels, which explains the decrease in critical speed. Further increasing ζ/E_1 , as seen in Figure 10a, causes the curve of the critical speed as a function of the elastic parameter E_1/E_2 to reduce. Meanwhile by increasing the parameter K_1/K_2 as seen in Figure 10b, the curves of the critical sliding speed as a function of the elastic parameter increase.

It can be inferred that increasing the thermal conductivity parameter of the viscoelastic material reduces the effect of the elastic parameter on the system stability while increasing the relaxation time increases the effect of the elastic parameter.

The variation of the critical speed Va_2/k_2 as a function of the relaxation time parameter ζ/E_1 for the elastic parameters E_1/E_2 and thermal conductivity parameters K_1/K_2 for the sliding pairs are considered. For relatively small values of the elastic parameter E_1/E_2 , the resulting critical speed is higher and is significantly influenced by the relaxation time τ as shown in Figure 11a. The critical speed decreases as the relaxation time parameter ζ/E_1 is increased. This is because the phase angle δ is highly influenced by E_1/E_2 and ζ/E_1 according to Eq. (15). As the phase angle increases, the critical speed decreases.

Meanwhile, there are critical values of the relaxation time τ at which the critical speed starts to rise and fall for relatively small values of E_1/E_2 . For instance, when $E_1/E_2 = 0.002$, the

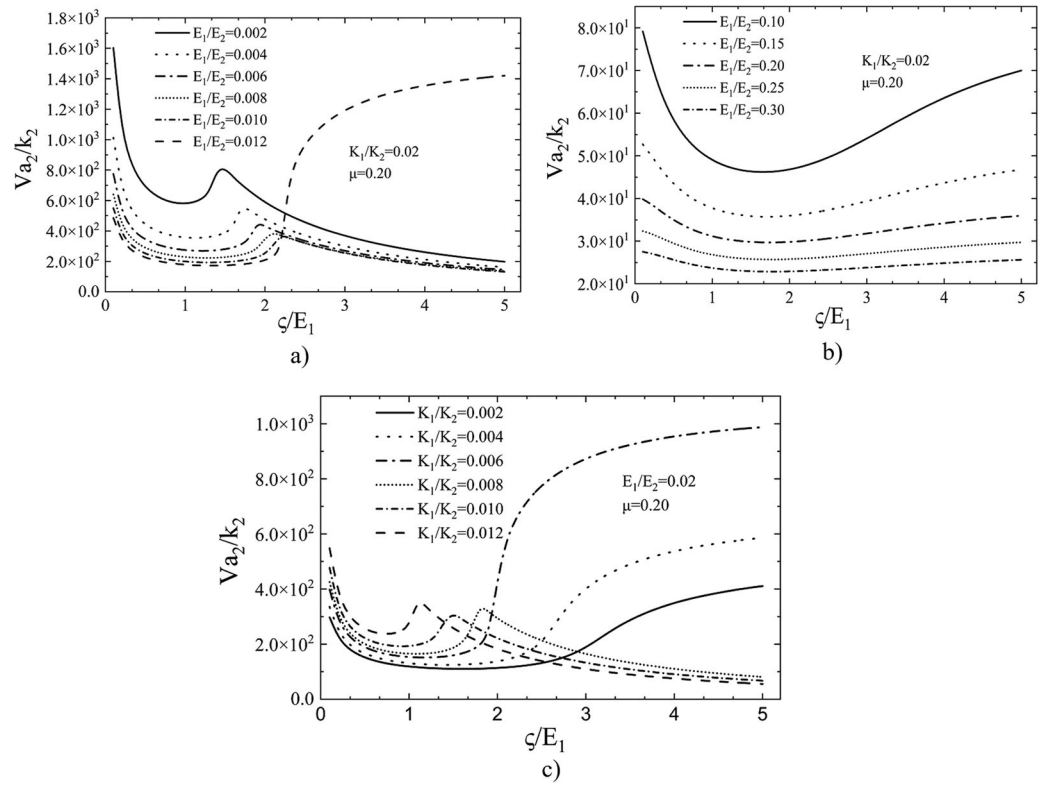


Figure 11. The variation of critical speed as a function of the relaxation time by considering different (a) smaller values of the elastic parameter, (b) larger values of the elastic parameter, and (c) values of the thermal conductivities.

normalized critical speed decreases rapidly from 1603.7 when $\zeta/E_1 = 0$ to 580.5 when $\zeta/E_1 = 1$. It then rises gradually to a localized peak of 808.5 when $\zeta/E_1 = 1.47$ and then starts decreasing gradually with an increasing ζ/E_1 . This trend is observed for all increasing values of the E_1/E_2 except when $E_1/E_2 = 0.012$. At $\zeta/E_1 > 1.91$ for $E_1/E_2 = 0.012$, a sharp rise in the critical speed is found. This further shows that there is a specific critical value above which increasing ζ/E_1 will cause the critical speed to rise. This occurs because as ζ/E_1 becomes larger and the phase angle approaches zero, the linear elastic problem is recovered. This may explain the sharp rise in critical speed as E_1/E_2 is increased to 0.012 when $\zeta/E_1 > 2$. Meanwhile, the curves start decreasing rapidly by further increasing E_1/E_2 with an oscillation trend as seen in Figure 11b. The profile becomes less pronounced and flattens to a more uniform profile as E_1/E_2 increases. This is caused by a shift in the phase angle, δ . When ζ/E_1 increases, the phase angle increases leading to a reduction in the critical speed. Conversely, by increasing the thermal conductivity parameter as seen in Figure 11c, the critical speed is improved. For small values of the thermal conductivity (0.01-0.04), increasing the ζ/E_1 above 2 causes the critical speed to increase rapidly. Meanwhile, when $K_1/K_2 > 0.04$ the reverse is observed. This could be because of the change in the phase angle δ . These phenomena observed for the viscoelastic friction material during sliding interactions are particularly useful in determining the threshold at which it can either stabilize noise and vibration or encourage the onset of instabilities.

5. Conclusion

A mathematical model is derived to predict the critical sliding speed of friction materials with viscoelastic parameters in automotive disk brakes and clutches. The model provides a means to



estimate the onset of instabilities for sliding interactions between a conducting material and a viscoelastic friction material, something that has yet to be extensively investigated. Moreover, a finite element approach to the problem is established to provide an alternative means to estimate the critical speed in viscoelastic friction materials and to validate the mathematical model. Three physical material parameters of viscoelastic friction materials are investigated: relaxation time ζ/E_1 , elastic parameter E_1/E_2 , and thermal conductivity parameter K_1/K_2 , and the following deductions are obtained:

- The relaxation time parameter is found to reduce the critical sliding speed of the system. This is strongly dependent on how the relaxation time impacts the phase angle, δ , during sliding. Meanwhile, for larger values of the relaxation parameter, the phase angle may approach zero. This means that the linear elastic solution is recovered, which may increase the critical sliding speed. Therefore, a viscoelastic friction pad material may either encourage or discourage the onset of instability depending on the resulting phase angle due to the relax-
- Increasing the elastic parameter significantly reduces the critical sliding speed, making the system susceptible to instability. Moreover, as the elastic parameter grows the resulting peak contact pressures and stresses increase, which also lead to thermomechanical instability.
- The thermal conductivity parameter significantly reduces the effect of the relaxation time and elastic parameters. Thus, increasing the critical speed and discouraging thermomechanical instability. It is determined that for a stable system while discouraging noise and vibration, a reasonable thermal conductivity ratio is required.

Generally, viscoelastic friction materials may either increase or decrease the critical sliding speed when used in automotive disk brakes and clutches. This is, however, dependent on the material property compositions. Therefore, a careful consideration of the appropriate combination and interaction of the elastic parameters and the thermal conductivity parameters is required for the manufacturing of viscoelastic friction materials in automotive disk brakes and clutches. Future work may include expanding the viscoelastic model to three dimensions to analyze antisymmetric geometries, consider the effects of wear coupled with viscoelasticity, and further investigate the effects of lubricated friction systems which employ viscoelastic materials.

Nomenclature

ω

half-thickness of the sliding layer i a_i b the growth rate of the perturbation E_i elastic modulus of the layer i k_i thermal diffusivity of layer i height of the layer i h_i thermal conductivity of the layer i K_i length of the sliding layer the wave number of the perturbation m number of hotspots n P_i pressure at the contact surface i sliding distance х T_o constant temperature Vthe sliding velocity of the layer V_{c_i} critical sliding speed of layer i damping modulus ζ δ the phase angle between stress and deformation relaxation time τ σ elastic stress coefficient of friction и

frequency of the cyclic load

- α_i coefficient of thermal expansion of layer i
- 1 suffix related to the friction layer
- 2 suffix related to the metal layer

Disclosure statement

No potential conflict of interest was reported by the author(s).

Funding

The authors are pleased to acknowledge support from the National Science Foundation under the contract (No. 1928876).

ORCID

Kingsford Koranteng (D) http://orcid.org/0000-0002-5369-4275 Cortney LeNeave (D) http://orcid.org/0000-0001-8011-2392 Yun-Bo Yi (D) http://orcid.org/0000-0001-9936-854X

References

- [1] G. Sathyamoorthy, R. Vijay, and D. Lenin Singaravelu, "Brake friction composite materials: A review on classifications and influences of friction materials in braking performance with characterizations," *Proc. Inst. Mech. Eng. Part J J. Eng. Tribol.*, vol. 236, no. 8, pp. 1674–1706, 2022. DOI: 10.1177/13506501211064082.
- [2] R. Vijay, D. Lenin Singaravelu, and R. Jayaganthan, "Development and characterization of stainless steel fiber-based copper-free brake liner formulation: A positive solution for steel fiber replacement," *Friction*, vol. 8, no. 2, pp. 396–420, 2020. DOI: 10.1007/s40544-019-0280-8.
- [3] E. Denys and A. Arbor, "Control of brake noise by tuned mass dampers," US2006/0266599A1, 2006.
- [4] A. Bajer, V. Belsky, and S.-W. Kung, *The Influence of Friction-Induced Damping and Nonlinear Effects on Brake Squeal Analysis*. Warrendale, PA, USA: SAE International, 2004, p. 9. DOI: 10.4271/2004-01-2794.
- [5] E. V. Torskaya and F. I. Stepanov, "Effect of surface layers in sliding contact of viscoelastic solids (3-D model of material)," *Front. Mech. Eng*, vol. 5, p. 26, 2019. DOI: 10.3389/fmech.2019.00026.
- [6] Z. P. Bažant, "2.02—Stability of elastic, anelastic, and disintegrating structures, and finite strain effects: An overview," in I. Milne, R.O. Ritchie, and B. Karihaloo, Eds. *Comprehensive Structural Integrity*, Oxford: Pergamon, 2000, pp. 47–80. DOI: 10.1016/B0-08-043749-4/02094-2.
- [7] L. Tessitore, "Damping Backplate Vibration in a Drum Brake," GB2346421A, 2000.
- [8] V. P. Sergienko, S. N. Bukharov, and A. V. Kupreev, "Noise and vibration in brake systems of vehicles. Part 1: Experimental procedures," *J. Frict. Wear*, vol. 29, no. 3, pp. 234–241, 2008. DOI: 10.3103/S106836608030136.
- [9] K. Koranteng, J.-S. Shaahu and Y.-B. Yi, "Effect of contact geometry on temperature field distribution and thermal buckling of an in-wheel disc brake system," *Aust. J. Mech. Eng.*, pp. 1–13, 2021. DOI: 10.1080/14484846.2021.1958992.
- [10] A. M. Al-Shabibi and J. R. Barber, "Transient solution of a thermoelastic instability problem using a reduced order model," *Int. J. Mech. Sci.*, vol. 44, no. 3, pp. 451–464, 2002. DOI: 10.1016/S0020-7403(01)00110-2.
- [11] F. F. Mahmoud, A. G. El-Shafei, A. E. Al-Shorbagy, and A. A. Abdel Rahman, "Effect of the material parameters on layered viscoelastic frictional contact systems," *Adv. Tribol.*, vol. 2010, pp. 1–14, 2010. DOI: 10.1155/2010/258307.
- [12] P. Decuzzi, "Frictionally excited thermoelastic instability in viscoelastic and poroelastic media," *Int. J. Mech. Sci.*, vol. 44, no. 3, pp. 585–600, 2002. DOI: 10.1016/S0020-7403(01)00101-1.
- [13] H. Yu, Z. Li and Q. Jane Wang, "Viscoelastic-adhesive contact modeling: Application to the characterization of the viscoelastic behavior of materials," *Mech. Mater.*, vol. 60, pp. 55–65, 2013. DOI: 10.1016/j.mechmat.2013.01.004.
- [14] J. Úradníček, M. Musil, L. Gašparovič, and M. Bachratý, "Influence of material-dependent damping on brake squeal in a specific disc brake system," Appl. Sci., vol. 11, no. 6, pp. 2625, 2021. DOI: 10.3390/ app11062625.



- Y. Zhao, H. Liu, N. Wang, B. Fan, and M. Li, "Friction analysis of anisotropic surface for viscoelastic mate-[15] rial," ILT, vol. 73, no. 8, pp. 1113-1121, 2021. DOI: 10.1108/ILT-06-2021-0223.
- [16] B. N. J. Persson, "On the elastic energy and stress correlation in the contact between elastic solids with randomly rough surfaces," J Phys. Condens Matter, vol. 20, pp. 312001, 2008. DOI: 10.1088/0953-8984/20/31/
- B. N. J. Persson, "Theory of rubber friction and contact mechanics," J Chem Phys, vol. 115, pp. 22, 2001. [17]
- [18] C. Feng, D. Zhang, K. Chen, and Y. Guo, "Study on viscoelastic friction and wear between friction linings and wire rope," Int. J. Mech. Sci., vol. 142-143, pp. 140-52, 2018. DOI: 10.1016/j.ijmecsci.2018.04.046.
- C.-Y. Lin, "Alternative form of standard linear solid model for characterizing stress relaxation and creep: [19] Including a novel parameter for quantifying the ratio of fluids to solids of a viscoelastic solid," Front. Mater, vol. 7, p. 11, 2020. DOI: 10.3389/fmats.2020.00011.
- N. Mills, M. Jenkins, and S. Kukureka, "Viscoelastic behaviour," in N. Mills, M. Jenkins, and S. Kukureka, [20] Eds. Plastics, 4th ed., Oxford. UK: Butterworth-Heinemann, 2020, pp. 111-25. DOI: 10.1016/B978-0-08-102499-7.00007-2.
- R. A. Burton, V. Nerlikar, and S. R. Kilaparti, "Thermoplastic instability in a seal-like configuration," Wear, [21] vol. 24, pp. 177-188, 1973,
- W. N. Findley, J. S. Lai, and K. Onaran, Creep and Relaxation of Nonlinear Viscoelastic Materials, With an [22] Introduction to Linear Viscoelasticity. Amsterdam/New York/Oxford: North-Holland Publishing Company; New York: Sole Distributors for the U.S.A. and Canada: Elsevier/North Holland INC, 1976,
- K. Koranteng, J.-S. Shaahu, and Y.-B. Yi, "A transient simulation of thermomechanical instability in metalfree friction materials with anisotropic properties," Int. J. Solids Struct., vol. 252, pp. 111816, 2022. DOI: 10. 1016/j.ijsolstr.2022.111816.
- M. Smith, ABAQUS/Standard User's Manual, Version 6.9. Providence, RI, USA: Dassault Systèmes Simulia [24] Corp, 2009.
- [25] J. C. Heinrich, P. S. Huyakorn, O. C. Zienkiewicz, and A. R. Mitchell, "An 'upwind' finite element scheme for two-dimensional convective transport equation," Int. J. Numer. Meth. Engng, vol. 11, no. 1, pp. 131-143, 1977. DOI: 10.1002/nme.1620110113.
- C.-C. Yu and J. C. Heinrich, "Petrov-Galerkin method for multidimensional, time-dependent, convective-[26] diffusion equations," Int. J. Numer. Meth. Eng., vol. 24, no. 11, pp. 2201-2215, 1987. DOI: 10.1002/nme.
- P. Zagrodzki, K. B. Lam, E. Al Bahkali, and J. R. Barber, "Nonlinear transient behavior of a sliding system [27] with frictionally excited thermoelastic instability," J. Tribol., vol. 123, no. 4, pp. 699-708, 2001. DOI: 10. 1115/1.1353180.